

# Accepted Manuscript

Size and temporal-dependent efficacy of oltipraz-loaded PLGA nanoparticles for treatment of acute kidney injury and fibrosis

Hang Yu, Tingsheng Lin, Wei Chen, Wenmin Cao, Chengwei Zhang, Tianwei Wang, Meng Ding, Sheng Zhao, Hui Wei, Hongqian Guo, Xiaozhi Zhao



PII: S0142-9612(19)30467-3

DOI: <https://doi.org/10.1016/j.biomaterials.2019.119368>

Article Number: 119368

Reference: JBMT 119368

To appear in: *Biomaterials*

Received Date: 15 January 2019

Revised Date: 8 July 2019

Accepted Date: 14 July 2019

Please cite this article as: Yu H, Lin T, Chen W, Cao W, Zhang C, Wang T, Ding M, Zhao S, Wei H, Guo H, Zhao X, Size and temporal-dependent efficacy of oltipraz-loaded PLGA nanoparticles for treatment of acute kidney injury and fibrosis, *Biomaterials* (2019), doi: <https://doi.org/10.1016/j.biomaterials.2019.119368>.

This is a PDF file of an unedited manuscript that has been accepted for publication. As a service to our customers we are providing this early version of the manuscript. The manuscript will undergo copyediting, typesetting, and review of the resulting proof before it is published in its final form. Please note that during the production process errors may be discovered which could affect the content, and all legal disclaimers that apply to the journal pertain.

1 Size and Temporal-Dependent Efficacy of Oltipraz-  
2 loaded PLGA Nanoparticles for Treatment of Acute  
3 Kidney Injury and Fibrosis

4  
5 *Hang Yu<sup>1,2#</sup>, Tingsheng Lin<sup>1,2#</sup>, Wei Chen<sup>1,2</sup>, Wenmin Cao<sup>1,2</sup>, Chengwei Zhang<sup>1,2</sup>, Tianwei Wang<sup>1,2</sup>,*  
6 *Meng Ding<sup>1,2</sup>, Sheng Zhao<sup>3</sup>, Hui Wei<sup>3\*</sup>, Hongqian Guo<sup>1,2\*</sup>, Xiaozhi Zhao<sup>1,2\*</sup>*

7  
8 1. Department of Urology, Nanjing Drum Tower Hospital, Medical School of Nanjing University,  
9 Institute of Urology, Nanjing University, Nanjing, Jiangsu 210008, China

10 2. Institute of Urology, Nanjing University, Nanjing, Jiangsu 210008, China

11 3. Department of Biomedical Engineering, College of Engineering and Applied Sciences, Nanjing  
12 National Laboratory of Microstructures, Jiangsu Key Laboratory of Artificial Functional Materials,  
13 Nanjing University, Nanjing, Jiangsu 210093, China

14  
15 # These authors contributed equally to this work.

16 \*Corresponding Authors: X. Zhao, Email: [zhaoxz@nju.edu.cn](mailto:zhaoxz@nju.edu.cn); H. Guo, Email: [dr.ghq@nju.edu.cn](mailto:dr.ghq@nju.edu.cn);

17 H. Wei, Email: [weihui@nju.edu.cn](mailto:weihui@nju.edu.cn).

18

19

20

21

22

**1 Abstract**

2 Acute kidney injury (AKI) is associated with high mortality and morbidity with no effective  
3 treatment available at present, which greatly escalates the risk of chronic kidney disease.  
4 Nanotechnology-based drug delivery for targeting renal tubules offers a new strategy for AKI  
5 treatment but remains challenging due to the glomerular filtration barrier. To tackle this challenge,  
6 here we demonstrate that poly (lactic-co-glycolic acid) (PLGA) nanoparticles (NPs) of 100 nm  
7 diameter could selectively accumulate in mouse injury kidneys in correlation to the degree of  
8 kidney injury and administration time during the initial phase of renal ischemia-reperfusion injury.  
9 The NPs were located in renal tubular epithelial cells confirmed by immunofluorescence, which is  
10 critical for the progression of AKI. Taking advantage of the high accumulation and renal tubule  
11 targeting of the PLGA NPs in the ischemia-reperfusion (IR) kidney, we designed PLGA NPs loaded  
12 with Oltipraz (PLGA-Oltipraz NPs) to treat IR-induced AKI and renal fibrosis. *In vitro* results  
13 showed that compared to free Oltipraz, PLGA-Oltipraz NPs displayed a higher antioxidation effect  
14 with improved cell viability, lower contents of malondialdehyde, and higher activity of superoxide  
15 dismutase. The therapeutic efficacy of PLGA-Oltipraz NPs was further investigated *in vivo*. Mice  
16 with AKI treated with PLGA-Oltipraz NPs exhibited significantly reduced tubular necrosis, less  
17 collagen deposition, and better renal function at the initial phase as well as improved renal fibrosis  
18 at the recovery phase. This study establishes a promising approach for AKI and fibrosis treatment  
19 with PLGA-Oltipraz NPs. It also reveals the importance of size-selective NPs and drug  
20 administration time window to nanotherapeutics.

21

**22 Keywords**

23 Drug delivery; Nanomedicine; Acute renal injury; Renal fibrosis; Nanoparticles

24

25

## 1 **1. Introduction**

2 Acute kidney injury (AKI) is a common and serious clinical disorder with high morbidity and  
3 mortality[1-3]. It occurs in 3.2% to 9.6% of hospitalized patients and is responsible for about 2  
4 million deaths per year worldwide with increasing incidence[4]. AKI causes microcirculatory  
5 disturbances, excessive production of reactive oxygen species and inflammatory factors, which  
6 give rise to the renal tubular injury[5-6]. This further stimulates the activation of interstitial  
7 fibroblasts, triggers extracellular matrix deposition in the interstitium, results in renal fibrosis, and  
8 eventually leads to chronic kidney disease (CKD)[7-8]. AKI, while has attracted much attention  
9 from nephrologists, still lacks specific and effective clinical treatments[9].

10

11 The development of nanotechnology sheds light on AKI treatment[10-11]. The nanoparticles  
12 (NPs)-based delivery system contributes to the pharmacokinetics and bio-distribution of drugs and  
13 facilitates targeted drug delivery to specific organs[12-15]. However, the use of the NPs-based  
14 system to deliver drugs to renal tubules is challenged by the glomerular filtration barrier (GFB)[16-  
15 17]. Under the physiological condition, water and small solutes (such as urea and glucose) in  
16 plasma are able to cross the GFB into the urine, while high-molecular-weight plasma components  
17 are retained in the blood[18]. Only a few nanomaterials were reported to target renal tubules. For  
18 instance, carbon nanotubes with a diameter of 5 nm were used for targeted drug delivery to renal  
19 tubules in a cisplatin-induced AKI model[19]. The carbon nanotubes loaded with Trp53 siRNA and  
20 Mep1b siRNA could effectively alleviate kidney damage and renal tubular inflammation. Catechol-  
21 derived chitosan NPs with a diameter of 40 nm could target renal tubules and interstitium, reducing  
22 the occurrence of renal fibrosis in the unilateral ureteral occlusion model[20]. Shaped DNA  
23 origami nanostructures had superiority of accumulation in mice kidneys. Besides, rectangular DNA  
24 origami nanostructures possessed renal-protective properties in AKI mouse model[21].  
25 Nevertheless, these materials are still far away from clinical application. More effective

1 nanomaterials for targeting renal tubules are required.

2

3 Renal ischemia-reperfusion injury (RIRI) is one of the most frequent causes of AKI[22].

4 Previous reports showed that the structure and permeability of GFB were significantly changed in  
5 the RIRI animal model at the initial phase, which may allow for NPs to pass through[23-25].

6 Therefore, we reasoned that it would be possible to design NPs with a specific size to cross the  
7 impaired GFB, which would in turn enable the targeted drug delivery to renal tubules. In the

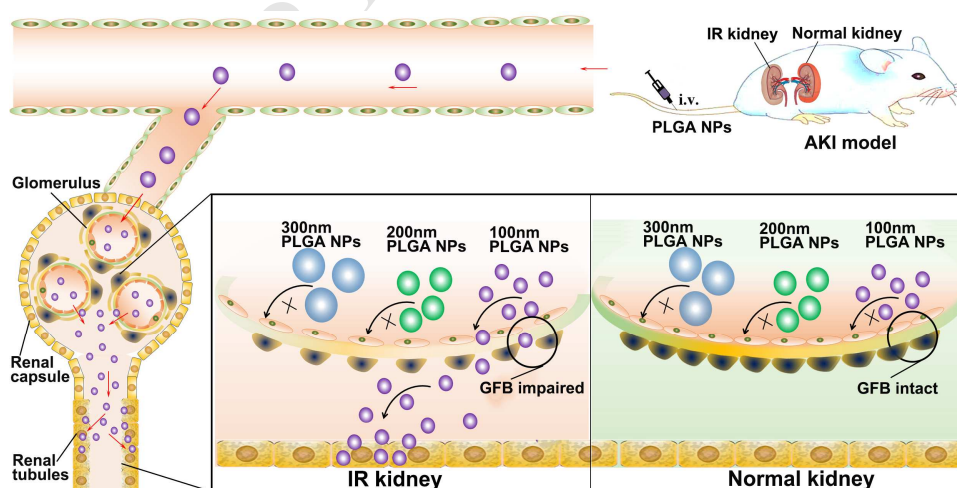
8 present study, taking poly (lactic-co-glycolic acid) (PLGA) as the model, we found that PLGA NPs  
9 of 100 nm could accumulate in the ischemia-reperfusion (IR) kidney and target renal tubular

10 epithelial cells at a specific administration time. The NPs accumulation was closely related to the  
11 degree of kidney injury and administration time of NPs. To further validate our hypothesis, we

12 loaded Oltipraz, a drug for AKI and renal fibrosis treatment, into PLGA NPs of 100 nm to prepare  
13 the PLGA-Oltipraz NPs, which were intravenously delivered to the IR-induced AKI-to-CKD

14 mouse model[26-28]. We found that the PLGA-Oltipraz NPs could specifically target the IR kidney  
15 at the initial phase and continuously release Oltipraz for effective treatment of AKI and renal

16 fibrosis (Scheme 1).



17

18 **Scheme 1. Application of PLGA-Oltipraz nanoparticles (NPs) with particle size of 100 nm in**

19 **ischemia-reperfusion (IR) induced acute kidney injury (AKI). GFB, glomerular filtration**

1 barrier; i.v., intravenous injection.

2

## 3 **2. Materials and methods**

### 4 **2.1. Fabrication of PLGA NPs**

5 The PLGA NPs of about 100 nm in diameter were prepared as follows[29-30]. 5 mg PLGA  
6 (Poly(D,L-lactide-co-glycolide) (lactide:glycolide 50:50, ester terminated, molecular weight is  
7 38,000-54,000, Sigma-Aldrich, St. Louis, MO, USA) was dissolved in acetonitrile (2 mL). DiR  
8 (Thermo Fisher Scientific, MA, USA), a cytomembrane dye, was then added to PLGA acetonitrile  
9 solution. Lecithin (soybean, refined, molecular weight: ~330 D) and DSPE-PEG (1,2-distearoyl-  
10 sn-glycero-3-phosphoethanolamine-N-carboxy(polyethylene glycol) 2000) were purchased from  
11 Sigma-Aldrich (St. Louis, MO, USA). Lecithin (1.5 mg) and DSPE-PEG (5 mg) were dissolved in  
12 20 mL of distilled water. Then the PLGA and DiR mixed acetonitrile solution was slowly added  
13 dropwise to the rapidly stirred lecithin and DSPE-PEG solution. To evaporate the acetonitrile, we  
14 further stirred the obtained solution overnight at room temperature. Then the obtained NPs  
15 suspension was ultrafiltered by using a Millipore Amicon centrifuge tube (molecular weight ~100  
16 kD) and washed twice to completely remove the organic solvent. The obtained NPs solution was  
17 resuspended in PBS with a PLGA concentration of 5 mg/mL, then the PLGA NPs dispersion was  
18 stored at 4 °C.

19 In order to prepare PLGA NPs with the size about 200 nm, 10 mg PLGA was dissolved in 1  
20 mL acetonitrile solution. Lecithin (1 mg) and DSPE-PEG (2 mg) were dissolved in 20 mL of  
21 distilled water. Remaining steps were the same as for 100 nm PLGA NPs.

22 In order to prepare PLGA NPs with the size about 300 nm, 20 mg PLGA was dissolved in 1  
23 mL acetonitrile solution. Lecithin (0.5 mg) and DSPE-PEG (1 mg) were dissolved in 10 mL of  
24 distilled water. Remaining steps were the same as 100 nm PLGA NPs.

25

## 1 2.2. Preparation of PLGA-Oltipraz NPs

2 PLGA-Oltipraz NPs of 100 nm in diameter were prepared as follows. PLGA (5 mg) was dissolved  
3 in acetonitrile (2 mL). Oltipraz (25 µg, Selleck, Shanghai), a Nrf2 activator was added to 2 mL of  
4 PLGA acetonitrile solution and thoroughly mixed at room temperature. DSPE-PEG (5 mg) and  
5 Lecithin (1.5 mg) were dissolved in 20 mL of distilled water. Then the PLGA and Oltipraz  
6 acetonitrile solution was slowly added dropwise to the rapidly stirred lecithin and DSPE-PEG  
7 solution, and then stirred overnight at room temperature. The prepared nano-suspension was  
8 ultrafiltered, centrifuged by using a Millipore Amicon centrifuge tube (molecular weight 100 kD)  
9 and washed twice to completely remove the organic solvent. The obtained NPs solution was  
10 resuspended in 1 mL PBS to produce PLGA-Oltipraz NPs solution.

## 12 2.3. Characterization of PLGA and PLGA-Oltipraz NPs

13 The morphology and particle size of NPs were evaluated by transmission electron microscopy  
14 (TEM; Hitachi H-7650). Dynamic light scattering (DLS; Brookhaven Instruments Corp., USA) was  
15 employed to measure the hydrodynamic size and zeta potential of NPs. Oltipraz concentration and  
16 loading capacity of NPs were determined by UV-visible spectra with a UV-visible  
17 spectrophotometer (UV2450, Shimadzu Corp.).

## 19 2.4. *In vitro* cellular uptake behavior of PLGA NPs

20 Human renal tubular epithelial cell line (HK2) was purchased from Cell Bank of Shanghai  
21 Institutes for Biological Sciences. HK2 cells were cultured in DEME medium containing 10% fetal  
22 bovine serum (Wisent, Nanjing, China), 1% penicillin-streptomycin (Gibco, MA, USA) and  
23 incubated in 5% CO<sub>2</sub> at 37 °C in a water-saturated atmosphere. Cells were seeded in 6-well plates  
24 with a density of 5×10<sup>5</sup> cells/well, and cultured for 24 h. To evaluate the cellular uptake of PLGA  
25 NPs by flow cytometry, fresh medium containing 1mg PLGA NPs (labeled with DiR, 2.5 µg/mL)

1 with different sizes were added. After 6 h co-incubation, cells were washed with phosphate  
2 buffered saline (PBS) three times and centrifuged, re-suspended in 500  $\mu$ L of PBS, and analyzed by  
3 flow cytometry. The fluorescence of DiR was collected on the APC-Cy7-H channel.

#### 4 5 **2.5. *In vitro* anti-oxidative stress effect of PLGA-Oltipraz NPs**

6 HK2 cells were seeded in two cell culture plates and cultured with DMEM containing 10% (v/v)  
7 FBS, pH 7.2, at 37 °C with 5% CO<sub>2</sub>. Cells were pre-treated separately with DMSO, PLGA NPs,  
8 PLGA-Oltipraz NPs, and free-Oltipraz, then cultured for 24 h. The concentration of Oltipraz in  
9 groups with free Oltipraz, and PLGA-Oltipraz NPs was 20  $\mu$ M. Cells in one plate were cultured in  
10 serum-starved medium and exposed to hypoxia for 1 h, then cultures were replaced with standard  
11 medium and allowed to recover in room air with 5% CO<sub>2</sub> for 1 h. Cells in another plate were  
12 cultured under normal conditions for 2 h. Cell lysates were prepared for subsequent experiments.  
13 Western blot analysis of the protein levels of Nrf2 (#12721, 1:1000, Cell Signaling Technology,  
14 Danvers, MA, USA), NQO1 (ab80588, 1:2000, Abcam, Cambridge, UK) and  $\alpha$ -Tubulin (sc-73242,  
15 1:5000, Santa Cruz). To examine malondialdehyde (MDA) and reactive oxygen species (ROS)  
16 generated by hypoxia condition, thiobarbituric acid was used to measure MDA, WST-8 assay kit  
17 (Beyotime Biotech, Shanghai, China) was used to examine ROS generation. And CCK-8 assay kit  
18 (Vazyme biotech, Nanjing, China) was used to assess cell viability. Briefly, cell lysis samples were  
19 first incubated with a working solution for an indicated time, followed by detection in a  
20 spectrophotometer system (TECAN). The total protein concentration of each sample was  
21 determined by the BCA Protein Assay Kit (Vazyme biotech, Nanjing, China), and was used to  
22 normalize the measured MDA and ROS results.

#### 23 24 **2.6. AKI-to-CKD mice model**

25 All animal experimental protocols were approved by the Institutional Animal Care and Use

1 Committee, Drum Tower Hospital, Medical School of Nanjing University. ICR Mice (6-8 weeks)  
2 were anesthetized with isoflurane inhalation, and injected buprenorphine subcutaneously for  
3 analgesia. AKI-to-CKD mice model was established by unilateral renal pedicle clamping for 45  
4 min followed by reperfusion as described previously[31]. In brief, we firstly removed the left renal  
5 hilus fat and isolated the renal vessels completely, then placed the mice on a 38 °C heating plate  
6 and clamped renal pedicle with vascular bulldog clamps for 45 min. Whereafter, we released the  
7 bulldog clamp slowly, and observed that the color of the left kidney changed from purple-black to  
8 red, indicating successful reperfusion. In the sham group, we isolate the left renal pedicle without  
9 clamping it.

10

### 11 **2.7. *In vivo* bio-distribution of PLGA NPs**

12 A PerkinElmer IVIS Spectrum small-animal *in vivo* imaging system was used to measure the  
13 fluorescence intensity of NPs. The near-infrared (NIR) fluorescent image parameters were preset by  
14 using DiR dye, with excitation wavelength at 745 nm and emission wavelength at 800 nm. The  
15 fluorescence intensity of the images was normalized.

16 To study the relation between NPs size and their bio-distribution, DiR labeled PLGA NPs  
17 (200  $\mu$ L, 5 mg/mL PLGA) of the three different particle sizes was intravenously injected in the  
18 RIRI mouse model immediately after RIRI. Three mice from each group were sacrificed by CO<sub>2</sub>  
19 asphyxiation at 3, 6, 12, 24, and 48 h after injection. Hearts, livers, spleens, lungs, and kidney  
20 tissues were removed and the surface of the organs was floated/cleaned with physiological saline,  
21 then blotted dry. The organs were photographed and the NIR fluorescent signals were measured.

22 To investigate the effect of NPs administration timing on NPs bio-distribution, RIRI mice  
23 were divided into six groups with different timing of NPs administration. DiR labeled NPs (200  $\mu$ L,  
24 5 mg/mL PLGA) was administered at 0 h, 12 h, 24 h, 48 h, and 72 h and 7 d after RIRI. Three mice  
25 from each group were sacrificed at 3, 6, 12, 24, and 48 h after injection, and then the major organs

1 were removed to perform NIR imaging.

2 To explore the relationship between the degree of injury in the RIRI kidney and the  
3 accumulation of NPs, mice were divided into four groups by the blocking time of the left kidney  
4 vessels: 15, 30, 45, and 60 min. DiR labeled NPs (200  $\mu$ L, 5 mg/mL PLGA) was intravenously  
5 injected immediately after RIRI. Three mice from each group were sacrificed at 3, 6, 12, 24 and 48  
6 h after injection. The major organs were then harvested for NIR imaging.

7

## 8 **2.8. Location of the accumulated PLGA NPs in injured kidney**

9 To revalidate that the PLGA NPs can target the IR kidney, IR kidneys with NPs accumulation  
10 illustrated by the *in vivo* imaging system were fixed in OCT gel and frozen at -20 °C, and frozen  
11 sections of 5- $\mu$ m thick were prepared. Then, tissue sections were incubated with 3% bovine serum  
12 albumin (BSA)/0.3% Triton X-100 for 15 min at room temperature. After removing the solution,  
13 sections were incubated at room temperature with fluorescein-labeled *Phaseolus vulgaris*  
14 erythroagglutinin (PHA-E (1:200), FL-1121, Vector Laboratories, Peterborough, UK) or *Arachis*  
15 *hypogaea* lectin (PNA (1:100), L7381, Sigma-Aldrich, St. Louis, MO, USA) for 1 h. After rinsing  
16 with PBS three times, the core was incubated with 4', 6-dia- midino-2-phenylindole (DAPI,  
17 Beyotime Biotechnology, Shanghai), and fluorescence was observed by fluorescence microscope.

18

## 19 **2.9. Therapeutic efficacy of PLGA-Oltipraz NPs in the AKI-to-CKD mice model**

20 In the established ischemia reperfusion induced AKI model, the mice were divided into eight  
21 groups (9 mice/group) for treatment: Sham, Sham+PLGA NPs, Sham+Oltipraz, Sham+PLGA-  
22 Oltipraz NPs, IR, IR+PLGA NPs, IR+Oltipraz, and IR+PLGA-Oltipraz NPs. PBS, PLGA NPs,  
23 Oltipraz, and PLGA-Oltipraz NPs were intravenously injected in the Sham and IR groups  
24 immediately. The dose of Oltipraz in groups with free Oltipraz, and PLGA-Oltipraz NPs was 5  $\mu$ g.  
25 The day of administration was set as 12 h. Three mice in each group were executed on day 3, 7, and

1 42 (6 weeks). Kidneys and other primary organs were harvested for hematoxylin and eosin (H&E)  
2 staining. Tissue sections (5  $\mu$ m) were stained with H&E and Masson trichrome (Solarbio Life  
3 Sciences, Beijing). The staining results were measured and scored to assess the degree of injury.  
4 The final score reflected the degree of cast formation, tubular necrosis, loss of brush border, and  
5 tubular dilation in 10 randomly selected, non-overlapping fields (200 $\times$ ) as follows: 0, none; 1,  
6  $\leq$ 10%; 2, 11 to 25%; 3, 26 to 45%; 4, 46 to 75%; and 5,  $\geq$ 76%.

7 Kidney sections were also used for IHC staining to detect the expression of extracellular matrix  
8 proteins. IHC was performed using paraffin-embedded sections according to standard protocols of  
9 Cell Signaling Technology. The antibodies used for IHC were as follows:  $\alpha$ -smooth muscle actin  
10 ( $\alpha$ -SMA; Abcam, Cambridge, UK, ab5694, 1:3000), collagen I (Abcam, ab34710, 1:400), and  
11 fibronectin (Abcam, ab2413, 1:400) DAB (ZSGB-BIO, Beijing) was used as an HRP-specific  
12 substrate. Photographs of representative fields were captured under high-power magnification  
13 ( $\times$ 200) by using Leica LAS v4.12 software. The positive areas in each image were counted and  
14 analyzed with Image-Pro Plus v6.0.

## 16 **2.10. Western blot analysis**

17 To examine the expression of Nrf2 signalling pathway-associated proteins, protein was extracted  
18 from tissues and cells and underwent western blot analysis as previously described[32]. The  
19 antibodies used were as follows: Anti-Nrf2 antibody (Cell Signalling Technology, Danvers, MA,  
20 USA, #12721, 1:1000) , anti-NQO1 antibody (Abcam, ab80588, 1:2000), anti-Gpx2 antibody  
21 (Abcam, ab137431, 1:1000), anti-GCLC antibody (Proteintech, Rosemont, IL, USA, 12601-1-AP,  
22 1:2000), and anti- $\alpha$ -Tubulin antibody (Santa Cruz, sc-73242, 1:5000).

## 24 **2.11. Measurement of renal function**

25 To investigate the renal function protection effect of PLGA-Oltipraz NPs, the AKI mouse model

1 was established by blocking the left kidney blood vessel for 45 min and resecting the right kidney  
2 after the release of the left blood vessel clamp, while the sham group underwent the right kidney  
3 resecting without the left pedicle clamping. Then, the AKI mouse model and sham operation mice  
4 were divided into eight groups (5 mice/group) for treatment: Sham+PBS, Sham+PLGA NPs,  
5 Sham+Oltipraz, Sham+PLGA-Oltipraz NPs, IR+PBS, IR+PLGA NPs, IR+Oltipraz, and  
6 IR+PLGA-Oltipraz NPs. PBS, PLGA NPs, Oltipraz, and PLGA-Oltipraz NPs were intravenously  
7 injected in the Sham and AKI groups immediately. The dose of Oltipraz in groups with free  
8 Oltipraz, and PLGA-Oltipraz NPs was 5  $\mu\text{g}$ . After 24 h, mice were sacrificed and blood samples  
9 were harvested. The serum was separated by centrifuging blood samples and stored at  $-80\text{ }^{\circ}\text{C}$  until  
10 analysis of BUN and serum creatinine. BUN and creatinine assay kits were purchased from  
11 BioAssay System (Hayward, USA).

12

### 13 **2.12. Statistical analysis**

14 Statistical analysis involved two-sided Student's *t*-test for two groups and one-way ANOVA for  
15 multiple groups.  $P < 0.05$  was considered statistically significant.

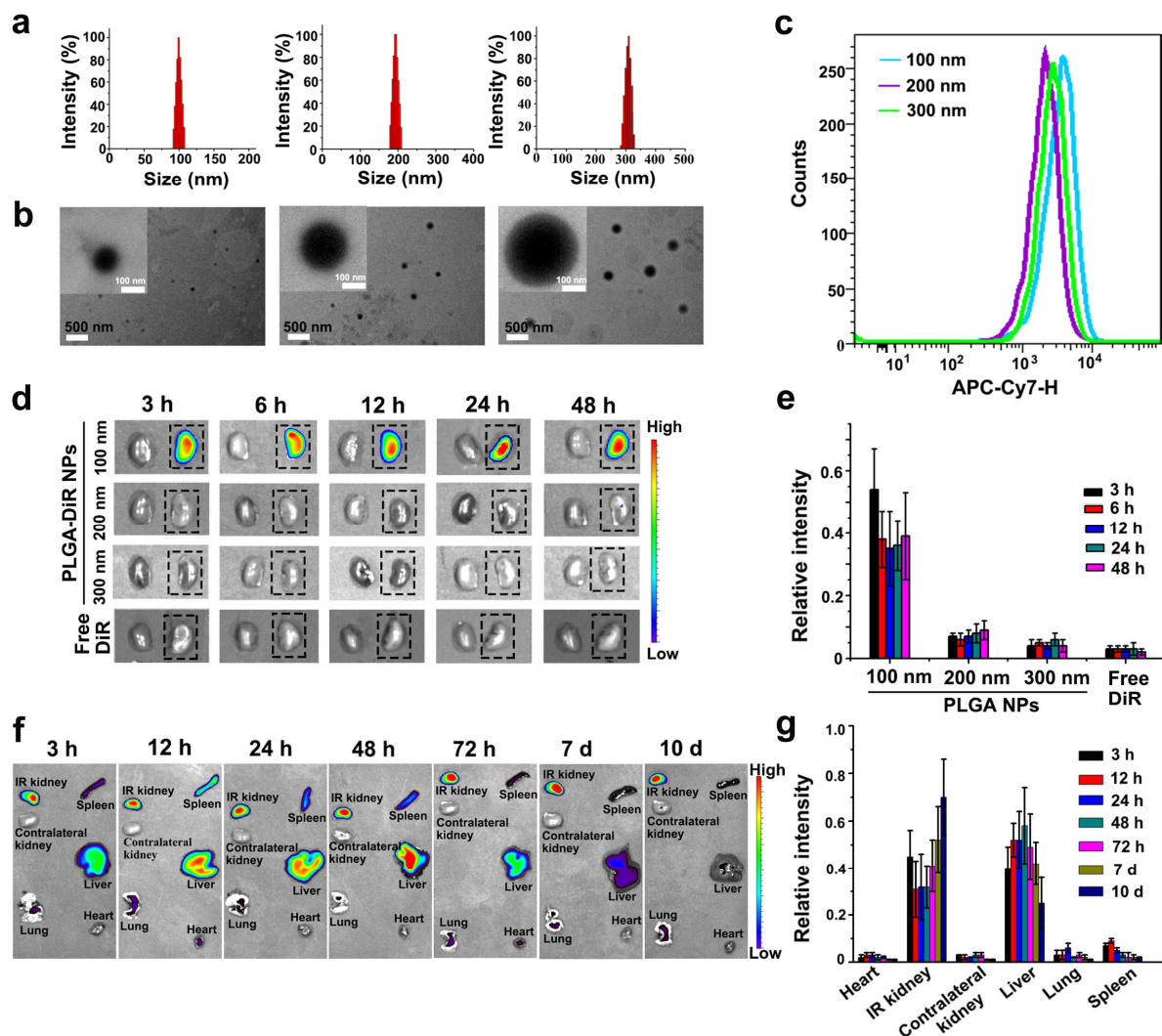
16

## 17 **3. Results and discussion**

### 18 **3.1. Characterization of PLGA NPs**

19 PLGA NPs with different particle size labeled with DiR were prepared. Fig. 1a-1c exhibits the  
20 particle size distribution, transmission electron microscope (TEM) images of different NPs, and the  
21 flow cytometry results of the obtained PLGA NPs in human renal tubular epithelial cells (HK2  
22 cells). Dynamic light scattering (DLS) showed that the mean size of the PLGA NPs fabricated at  
23 100, 200, and 300 nm was  $100 \pm 14.1$ ,  $200 \pm 19.5$  and  $300 \pm 20.8$  nm, respectively (Fig. 1a), and  
24 the PDI was  $0.098 \pm 0.009$ ,  $0.112 \pm 0.015$ , and  $0.156 \pm 0.027$ , respectively. TEM revealed that all  
25 the three NPs formed by self-assembly were generally spherical in shape and showed good mono-

1 dispersity (Fig. 1b). Next, we investigated the cellular uptake efficiency of PLGA NPs by  
 2 incubating HK2 cells with the three sizes of NPs for 4 h. The three PLGA-DiR NPs had similar  
 3 cellular uptake behaviors observed from flow cytometry (Fig. 1c).



4  
 5 **Figure 1. The characterization and *in vivo* bio-distribution of PLGA NPs.** (a) Size distribution  
 6 of PLGA NPs by dynamic light scattering. (b) Transmission electron microscopy (TEM) images of  
 7 PLGA NPs. Scale bar, 500 nm. (c) Flow cytometry of HK2 cells incubated with PLGA NPs of  
 8 different sizes. (d) PLGA NPs with different particle sizes and free DiR were intravenously injected  
 9 in renal ischemia-reperfusion injury (RIRI) model of mice immediately after surgery. NIR  
 10 fluorescence images of ischemia-reperfusion (IR) kidneys (dotted box) and contralateral kidneys of  
 11 RIRI mouse at the indicated time after injection. (e) Semi-quantitative bio-distribution of PLGA

1 NPs in IR kidneys from (d). (f) NIR fluorescence images of major organs after injection of PLGA  
2 NPs with particle size of 100 nm. (g) Semi-quantitative bio-distribution of PLGA NPs in RIRI  
3 mouse model by mean PLGA NPs fluorescence intensity in organs from (f). The data are shown as  
4 mean  $\pm$  SD (n=3).

5

### 6 **3.2. Bio-distribution of PLGA NPs**

7 We investigated the relationship between the particle size and their accumulation in the IR kidney  
8 after administration of PLGA-DiR NPs with three particle sizes. IR-induced AKI-to-CKD mouse  
9 model was established by unilateral renal pedicle clamping for 45 min followed by reperfusion as  
10 described previously[31]. PLGA-DiR NPs with the three different particle sizes (100 nm, 200 nm  
11 and 300 nm) and free DiR were intravenously injected immediately after the model was established,  
12 respectively. The near-infrared (NIR) fluorescence of the mouse IR kidney and contralateral kidney  
13 was observed at 3, 6, 12, 24, and 48 h post-injection. The semiquantitative analysis of NIR  
14 fluorescence in IR kidneys at 48 h post-injection showed that the relative fluorescence intensity of  
15 100 nm PLGA NPs, 200 nm PLGA NPs, 300 nm PLGA NPs and free DiR was 39%, 7%, 4% and  
16 2%, respectively. PLGA NPs of 100 nm significantly accumulated in IR kidneys, whereas NPs of  
17 200 and 300 nm were barely accumulated (Fig. 1d, e). Thus, the kidney-targeting property of PLGA  
18 NPs was closely related to particle size. On the other hand, all contralateral kidneys showed  
19 negligible DiR fluorescence. This was probably due to the impaired GFB after the RIRI, which  
20 enabled large molecules to pass through[33-34]. Meanwhile, the permeability of GFB at the  
21 contralateral kidney was not changed by RIRI. Therefore, PLGA NPs with different particle size  
22 could not accumulate in the contralateral kidneys. We also noted that no NIR fluorescence was  
23 detected in IR kidneys or contralateral kidneys after free DiR injection (Fig. 1d). The possible  
24 reason is still under investigation and will be reported in due course.

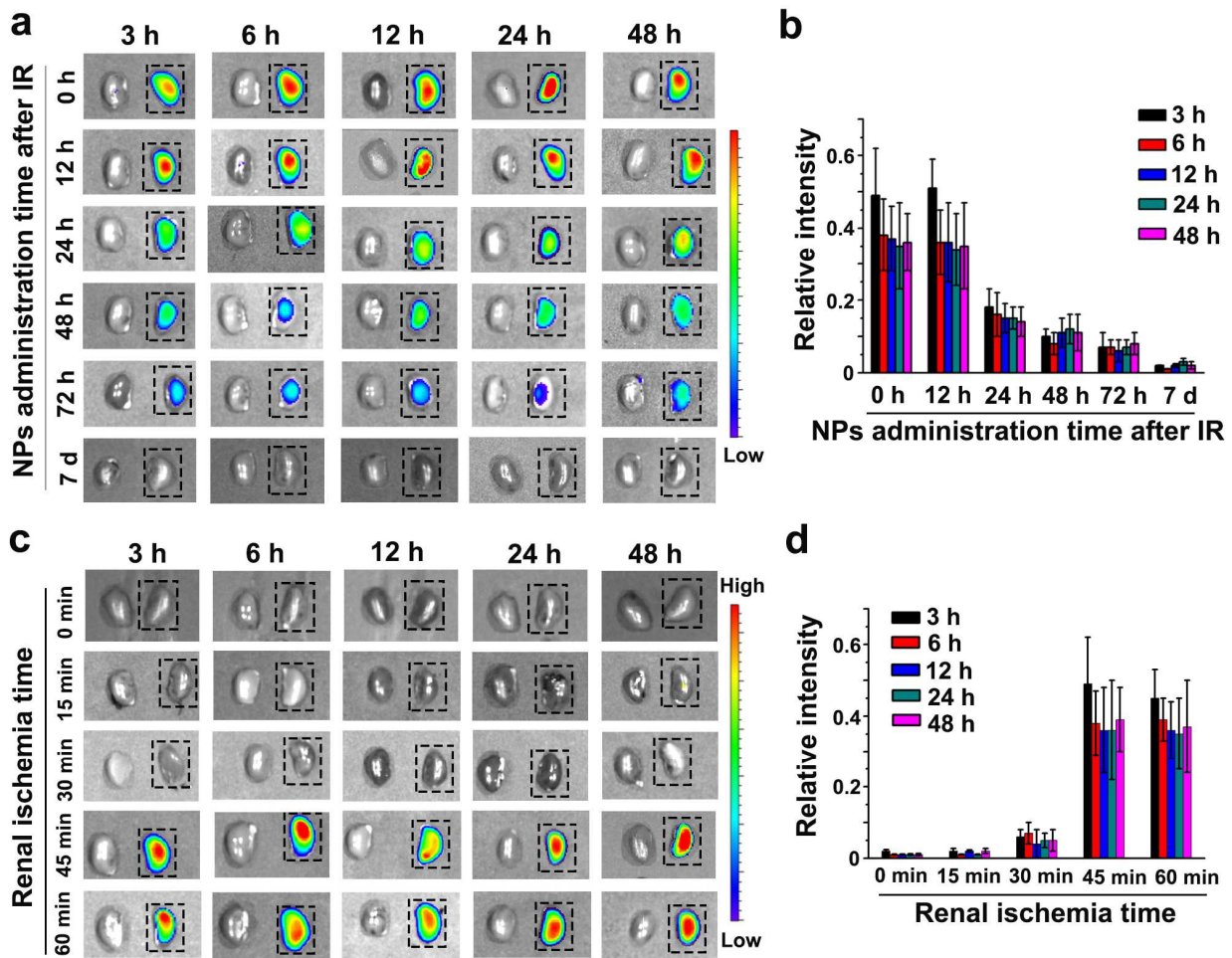
25

1 To evaluate the bio-distribution of PLGA NPs *in vivo*, we intravenously injected 200  $\mu$ L of  
2 100 nm PLGA NPs (0.05 mg/mL) in RIRI mice, and then imaged them by a NIR imaging system.  
3 Among major organs excised at different timepoints post-injection, strong DiR fluorescence  
4 intensity appeared in the IR kidney, whereas the contralateral kidney showed negligible DiR  
5 fluorescence (Fig. 1f). The relative fluorescence intensity in IR kidneys at 3 h, 12 h, 24 h, 48 h, 72  
6 h, 7 days and 10 days post-injection was 45%, 31%, 32%, 32%, 41%, 52% and 70%, respectively  
7 (Fig. 1g). The results revealed that PLGA NPs could specifically target the IR kidney. At day 10  
8 after injection, the fluorescence from PLGA NPs was still evident in IR kidney, indicating PLGA  
9 NPs could stay in the IR kidney for at least 10 days, thus enabling the continuous release of the  
10 encapsulated drugs.

11  
12 Next, we investigated the effect of administration timing on the accumulation of NPs in the IR  
13 kidney. The PLGA-DiR NPs of 100 nm were administered at 0 h, 12 h, 24 h, 48 h, 72 h, and 7 days  
14 after the establishment of the RIRI model. At 3, 6, 12, 24, and 48 h after administration, the major  
15 organs of mice were excised for NIR imaging. Fig. 2a exhibits the NIR fluorescence images of  
16 kidneys. At 48 h NIR imaging, the relative fluorescence intensity of IR kidney at 0, 12, 24, 48 and  
17 72 h NPs administration was 18, 17.5, 7, 5.5, and 4 times higher than that at 7 days NPs  
18 administration, respectively (Fig. 2a, b). The relative fluorescence intensity of IR kidney was  
19 significantly higher at 0 h and 12 h administration while gradually decreased with the delayed  
20 administration. Therefore, the accumulation of PLGA NPs in the IR kidney is reversely correlated  
21 with increased administration timing. Overall, substantial accumulation of NPs occurred even when  
22 the administration was given within 72 h after RIRI.

23  
24 We further explored the effect of the degree of injury of the IR kidney on the accumulation of  
25 NPs. The RIRI mice were divided into five groups by ischemic time of left kidneys: 0 (sham-

1 operated group), 15, 30, 45 and 60 min, respectively. The PLGA-DiR NPs of 100 nm were  
2 administered immediately after surgery, at 3, 6, 12, 24 and 48 h, the major organs of mice were  
3 excised for NIR imaging. The relative fluorescence intensity at 48 h in IR kidneys of 0, 15, 30, 45  
4 and 60 min ischemic time was 2%, 2%, 5%, 39%, and 37%, respectively. PLGA NPs accumulation  
5 was barely observed in groups with an ischemic time of 15 and 30 min, indicated by very low  
6 fluorescence intensity. However, with the ischemic time of 45 and 60 min, the accumulation of  
7 PLGA NPs in IR kidneys was significantly increased, reflected by the relatively high fluorescence  
8 intensity (Fig. 2c, d). We reason that the degree of injury is an important factor affecting the  
9 accumulation of NPs in IR kidneys. These results suggest that mild renal injury may not  
10 significantly change the structure and permeability of GFB and prevent the NPs from passing  
11 through. However, the kidney will get fully recovery from mild ischemia-reperfusion injury and  
12 will not progress to renal fibrosis.



1

2 **Figure 2. PLGA NPs bio-distribution by NIR imaging.** (a) The renal ischemia-reperfusion injury

3 (RIRI) mice were intravenously injected with 100 nm PLGA NPs at the indicated time (0, 12, 24,

4 48, 72 h and 7 d) after surgery. NIR fluorescence images of ischemia-reperfusion (IR) kidneys

5 (dotted box) and contralateral kidneys of RIRI mice at different times (3, 6, 12, 24, 48 h) after

6 injection. (b) Semi-quantitative bio-distribution of PLGA NPs in IR kidneys from (a). (c) PLGA

7 NPs with 100 nm particle sizes were intravenously injected in RIRI mice with different renal

8 ischemia time (0, 15, 30, 45, 60 min) immediately after surgery. NIR fluorescence images of IR

9 kidneys (dotted box) and contralateral normal kidneys at different times (3, 6, 12, 24, 48 h) after

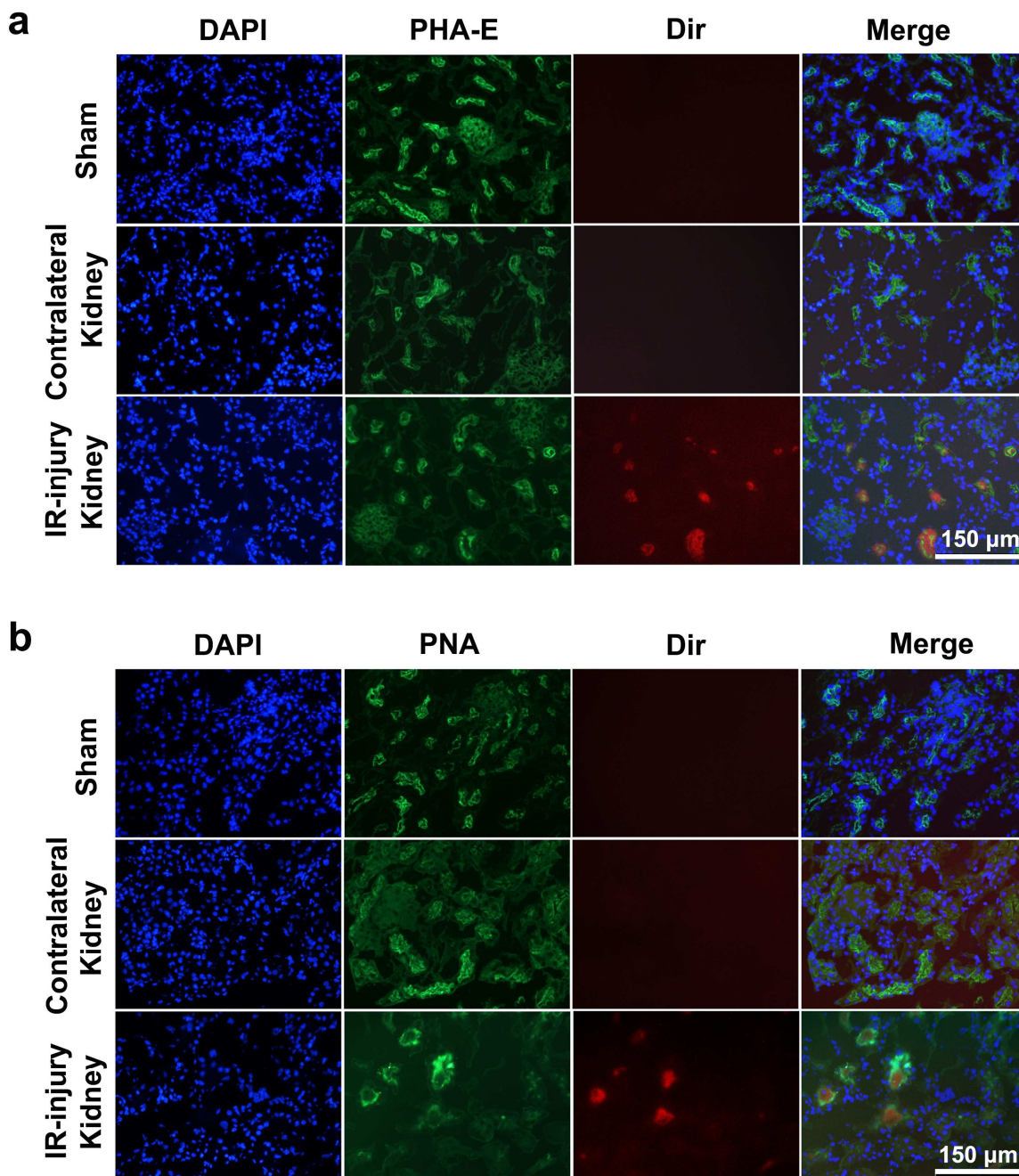
10 injection. (d) Semi-quantitative bio-distribution of PLGA NPs in IR kidneys from (c). The data are

11 shown as mean  $\pm$  SD (n=3).

12

### 1 **3.3. Localization of PLGA NPs**

2 We observed the accumulation of 100 nm PLGA NPs in the IR kidney. To further identify the exact  
3 location of PLGA NPs in the IR kidney, we applied immunofluorescence analysis to kidney frozen  
4 sections. IR kidney sections were stained with phytohemagglutinin-E (PHA-E) to label proximal  
5 convoluted tubules while phytoagglutinin (PNA) was used to label distal convoluted tubules,  
6 respectively[35]. DiR fluorescence was mainly observed in proximal and distal convoluted tubule  
7 cells in the IR kidney, while DiR fluorescence was negligible in the contralateral kidney or sham  
8 control kidney (Fig. 3a, b). It has been reported that renal tubular epithelial cells play important  
9 roles in the progression and recovery of AKI[7]. Tubular epithelial cells were observed to arrest at  
10 G2/M and adopt a profibrotic phenotype after AKI, leading to the progression of interstitial  
11 inflammation and fibrosis. Thus, repairing injured tubules to restore regular tubular function is of  
12 great significance in the treatment of AKI. In the present study, we demonstrated that PLGA-DiR  
13 NPs might directly target the proximal and distal convoluted tubules, which could contribute to  
14 drug delivery targeting the injured renal tubular epithelial cells.



1

2 **Figure 3. Immunofluorescence analysis of PLGA-DiR NPs in IR-injured and contralateral**  
 3 **kidneys.** PLGA-DiR NPs were intravenously injected immediately after RIRI or sham surgery in  
 4 mice. At 12 h after surgery, frozen kidney sections were prepared and stained with  
 5 phytohemagglutinin-E (PHA-E) for visualizing proximal tubules (a) and phytoagglutinin (PNA) for  
 6 visualizing distal tubules (b). DAPI was used for staining nuclei. Merged views are shown in the  
 7 right panels. Representative fluorescent images are from three independent experiments showing  
 8 similar results. Scale bar, 150  $\mu\text{m}$ .

1

### 2 **3.4. Fabrication and characteristics of PLGA-Oltipraz NPs**

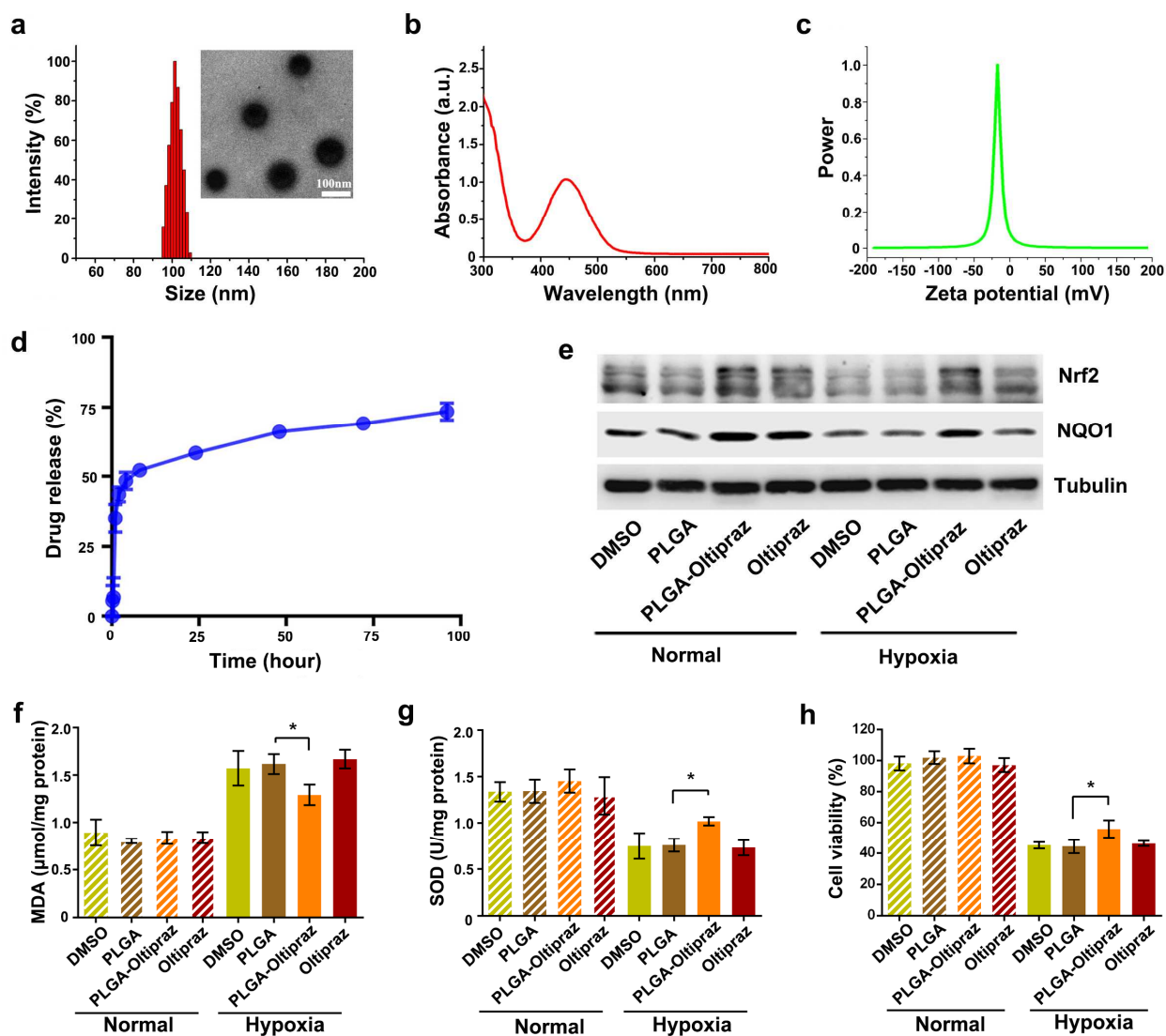
3 We then constructed PLGA NPs encapsulating Oltipraz by using the method for 100 nm PLGA NPs.  
4 Oltipraz, a small molecule Nrf2 (nuclear factor erythroid 1-related factor 2) agonist, was chosen as  
5 the model drug because it regulates cell oxidative stress damage and has huge potential in the  
6 treatment of AKI and renal fibrosis[26-28]. Nrf2 is a nuclear transcription factor which binds to  
7 antioxidant response element and participates in modulating transcription and expression of  
8 antioxidant enzymes[36-38]. Though Oltipraz can easily pass through the GFB, maintaining an  
9 effective concentration in the renal tubules and interstitium is difficult[39-40]. Herein we  
10 constructed Oltipraz-loaded PLGA NPs to address this challenge. DLS confirmed the mean size of  
11 the PLGA-Oltipraz NPs as  $100 \pm 15.8$  nm (Fig. 4a) with a PDI of  $0.109 \pm 0.012$ . TEM images  
12 showed that the self-assembled PLGA-Oltipraz NPs were generally spherical in shape. The UV-  
13 visible absorption spectrum of PLGA-Oltipraz NPs showed a characteristic absorption peak of  
14 Oltipraz at about 444 nm, indicating the successful encapsulation of Oltipraz (Fig. 4b). The loading  
15 capacity of Oltipraz was 1.1%. The zeta potential was  $-20 \pm 6.7$  mV (Fig. 4c). The release profile of  
16 Oltipraz from PLGA-Oltipraz NPs was evaluated. The cumulative release of Oltipraz reached 50%  
17 and 75% after 12 h and 4 days respectively, which indicated that drug release from PLGA NPs was  
18 a controlled-release process (Fig. 4d).

19

### 20 **3.5. Antioxidant efficacy of PLGA-Oltipraz NPs *in vitro***

21 Next, we inspected the antioxidation effect of PLGA-Oltipraz NPs *in vitro*. Western blot assay was  
22 performed to analyze the expression levels of Nrf2 and NQO1. Under normal culture conditions,  
23 compared with PLGA and the DMSO control, both the PLGA-Oltipraz NPs and Oltipraz could  
24 activate Nrf2 and NQO1 expression, with PLGA-Oltipraz NPs exhibiting higher activation  
25 efficiency than Oltipraz alone (Fig. 4e). Under hypoxia and serum-free culture conditions, the

1 expression of Nrf2 and NQO1 was inhibited. However, PLGA-Oltipraz and Oltipraz NPs conferred  
2 relatively higher expression of Nrf2 and NQO1 protein than the PLGA and DMSO control. The  
3 activation efficiency of the PLGA-Oltipraz NPs was better than Oltipraz alone in hypoxia and  
4 serum-free conditions. The malondialdehyde (MDA) content was 1.29  $\mu\text{mol}/\text{mg}$  protein in PLGA-  
5 Oltipraz treated cells, while 1.62  $\mu\text{mol}/\text{mg}$  protein in PLGA treated control cells ( $p < 0.05$ ) during  
6 hypoxia (Fig. 4f). The superoxide dismutase (SOD) activity showed 1.02 U/mg protein in PLGA-  
7 Oltipraz treated cells, while 0.76 U/mg protein in PLGA treated cells ( $p < 0.05$ ) in hypoxia (Fig.  
8 4g). Moreover, the cell viability rate was 44.36% and 55.81% in PLGA and PLGA-Oltipraz treated  
9 cells in hypoxia condition ( $p < 0.05$ ), respectively (Fig. 4h). PLGA-Oltipraz treatment conferred  
10 protection against hypoxia condition, as evidenced by lower contents of MDA, higher activity of  
11 SOD, and increased cellular activity when compared with PLGA and DMSO control cells (Fig. 4f,  
12 g, h).



1  
2 **Figure 4. Characterization of PLGA-Oltipraz NPs and their antioxidant role *in vitro*.** (a) Size  
3 distribution and colloid stability of PLGA-Oltipraz NPs by dynamic light scattering. Inset: TEM of  
4 PLGA-Oltipraz NPs; scale bar, 100 nm. (b) UV-visible absorption spectrum and (c) zeta potential  
5 of PLGA-Oltipraz NPs. (d) Oltipraz release profiles of PLGA-Oltipraz NPs. (e) HK2 cells were  
6 pretreated separately with PLGA-Oltipraz, PLGA, Oltipraz, and DMSO for 24 h. Normal group  
7 cells were cultured in standard medium and room air with 5% CO<sub>2</sub> for 2 h. Hypoxia group cells  
8 were cultured in medium without serum and exposed to hypoxia for 1 h, the cultures were replaced  
9 with standard medium and allowed to recover in room air with 5% CO<sub>2</sub> for 1 h. Western blot  
10 analysis of the effect of DMSO, PLGA, PLGA-Oltipraz or Oltipraz NPs on Nrf2 and downstream  
11 NQO1 (the protein levels were normalized to Tubulin level). (f) Malondialdehyde (MDA) levels by

1 thiobarbituric acid assay. (g) Reactive oxygen species (SOD) levels by WST-8 assay. (h) Cell  
2 viability by CCK-8 assay. \*P<0.05, t test.

3

### 4 **3.6. Therapeutic efficacy of PLGA-Oltipraz NPs *in vivo***

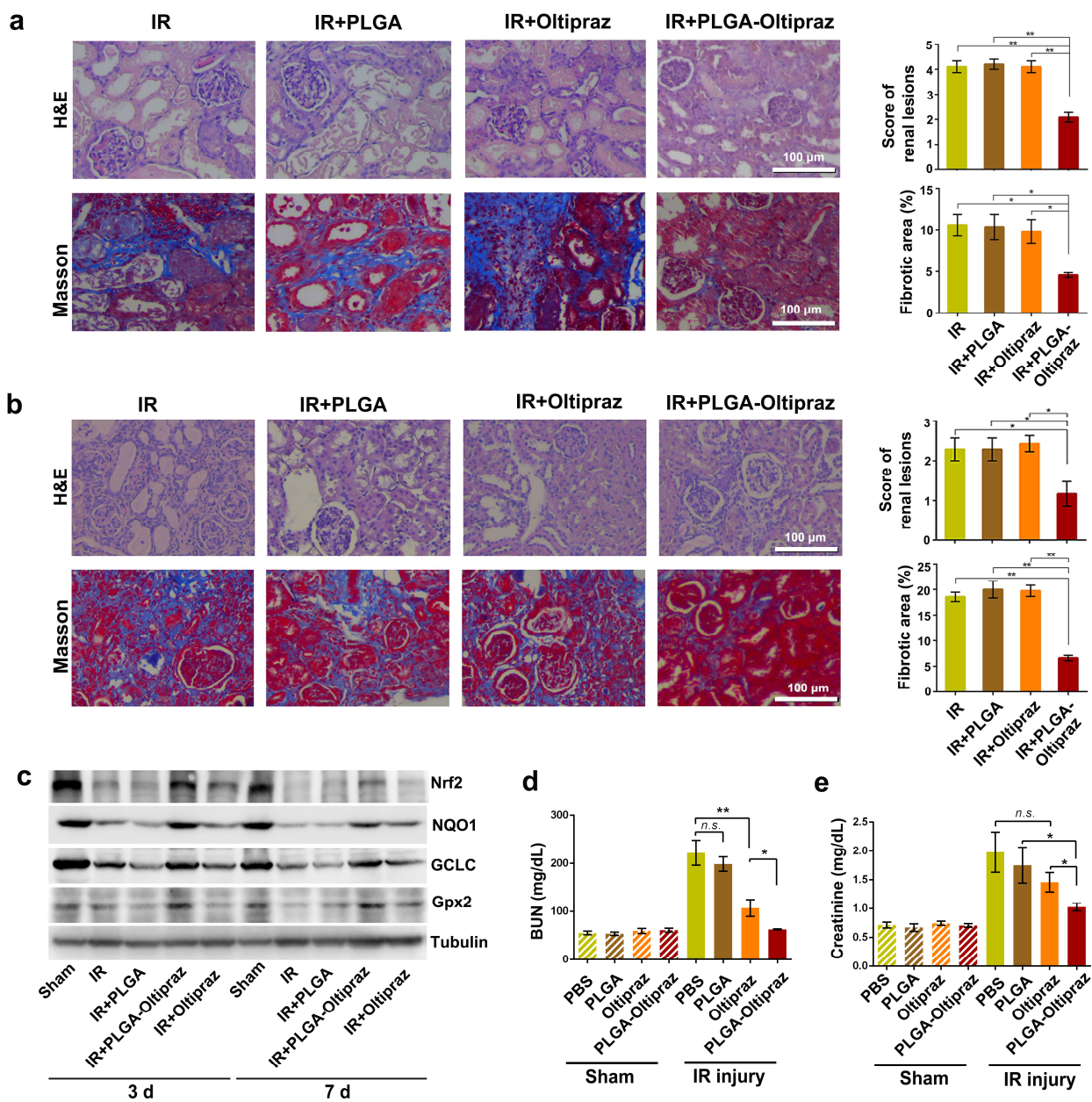
5 Having achieved substantially high accumulation of PLGA NPs of 100 nm in the IR kidney, we  
6 next investigated the therapeutic efficacy of PLGA-Oltipraz NPs *in vivo*. RIRI mice were divided  
7 into eight groups for treatment: IR, IR+PLGA NPs, IR+Oltipraz, IR+PLGA-Oltipraz NPs, sham,  
8 sham+PLGA NPs, sham+Oltipraz and sham+PLGA-Oltipraz NPs. Mice in sham group underwent  
9 renal pedicle isolation without clamping. On day 3 after IR injury, IR, IR+PLGA NPs, and  
10 IR+Oltipraz kidneys showed a significantly higher degree of tubular damage on H&E staining,  
11 including cast formation, tubular necrosis, loss of brush border, and dilatation of tubules. However,  
12 mice treated with PLGA-Oltipraz NPs showed less tubular damage and the score of renal lesions  
13 was significantly reduced (Fig. 5a), which suggests the protective effect of PLGA-Oltipraz NPs on  
14 IR-induced renal injury. We then assessed renal fibrotic lesion area by Masson staining. PLGA-  
15 Oltipraz NPs administration markedly reduced collagen accumulation and deposition in the renal  
16 tubular interstitium; the fibrotic area was significantly lower than that with other treatments (Fig.  
17 5a). To further determine the fibrotic lesions *in vivo*, we examined the expression of  $\alpha$ -SMA, a  
18 marker of fibroblasts, collagen I, and fibronectin, representing extracellular matrix proteins, in  
19 renal tissues by IHC staining (Fig. 6a). In the IR+PLGA-Oltipraz NPs group, the expression of  $\alpha$ -  
20 SMA, collagen I and fibronectin was significantly reduced (Fig. 6a). These results suggest a  
21 significant protective effect of PLGA-Oltipraz NPs on the IR kidney at the initial phase. Next, we  
22 further performed histological analysis of the IR kidneys at 6 weeks after RIRI and treatment. The  
23 score of renal fibrosis and fibrotic area (Fig. 5b), as well as  $\alpha$ -SMA, collagen I, and fibronectin  
24 positive areas were significantly lower with IR+PLGA-Oltipraz NPs than other administrations  
25 (Fig. 6b), which suggests the anti-fibrosis function of PLGA-Oltipraz NPs in the late stage of RIRI

1 pathogenesis. Meanwhile, we performed histological analysis of the sham-operated groups and  
2 found no significant difference in H&E, Masson, and IHC staining between each group (Figure S1).

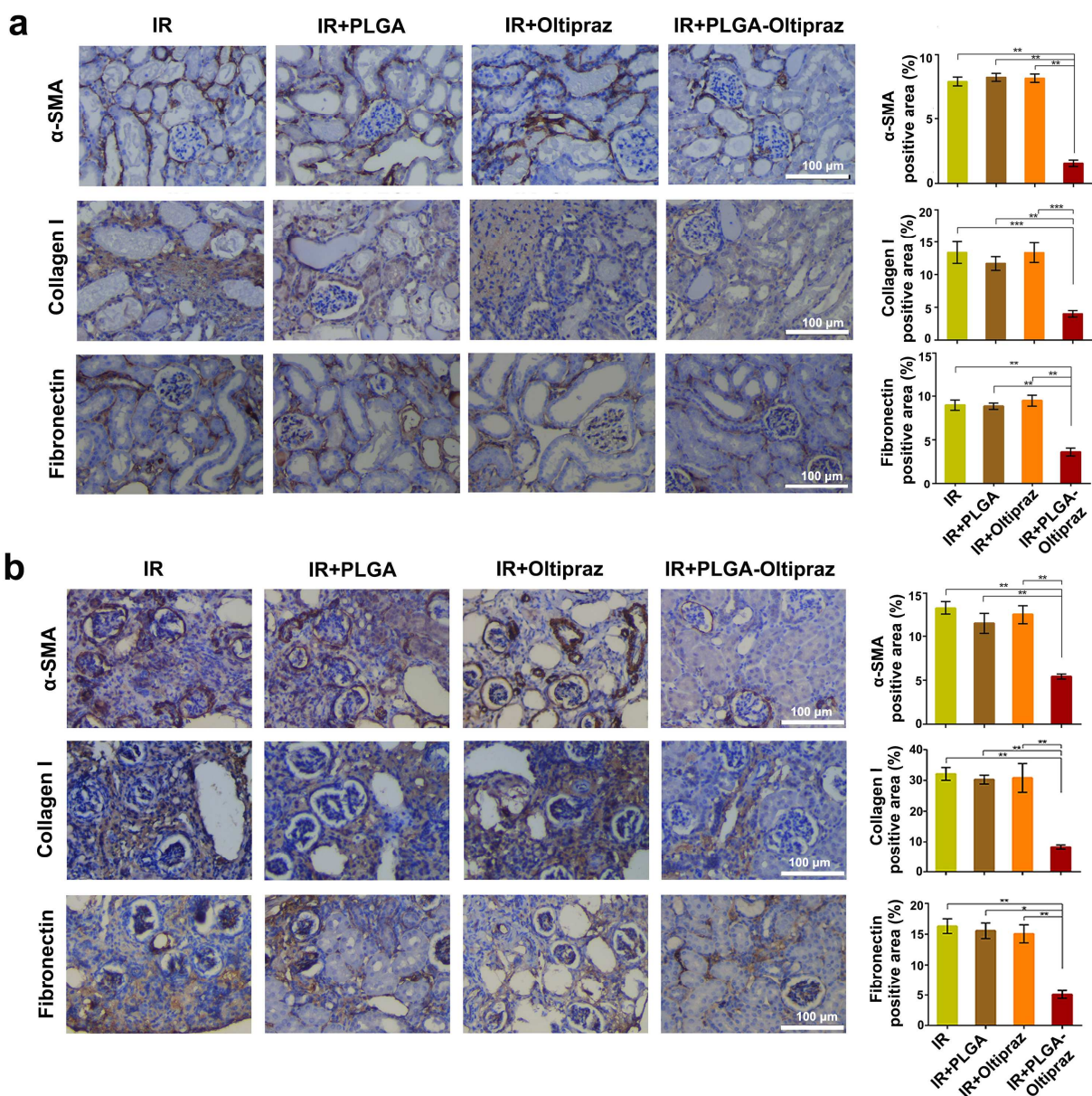
3  
4 The expression of Nrf2 signaling pathway-associated proteins were also examined in kidney  
5 tissues. On days 3 and 7 after RIRI, the IR kidneys of five groups were harvested for western blot  
6 analysis. Apart from the high expression of Nrf2 and its downstream proteins in the sham group,  
7 renal IR injury could inherently inhibit the Nrf2 signaling pathway at days 3 and 7 after RIRI (Fig.  
8 5c). Oltipraz is a strong Nrf2 activator, however, the activation effect of Oltipraz alone was slight.  
9 The expression of Nrf2 and its downstream proteins showed great increase with PLGA-Oltipraz  
10 NPs administration, suggesting that Nrf2 signaling pathway could be activated by the PLGA-  
11 Oltipraz NPs. Nrf2 is responsible for regulating the cell's antioxidant response via the antioxidant  
12 response element and is thought to be involved in the repair and recovery process from AKI[41].

13  
14 What's more, we evaluated the renal function protection effect of PLGA-Oltipraz NPs in RIRI  
15 mice with right kidney dissection. After establishing the RIRI model, PBS, PLGA NPs, Oltipraz,  
16 and PLGA-Oltipraz NPs were intravenously injected immediately in the sham control group and  
17 AKI group. Both serum creatinine and blood urea nitrogen (BUN) levels were increased 24 h after  
18 RIRI (Fig. 5d, e). In hypoxia condition, the BUN content was 222.16 mg/dL and 198.85 mg/dL  
19 respectively in PBS and PLGA added cells. Serum BUN level was decreased to 107.28 mg/dL in  
20 Oltipraz group compare to that in PBS control group ( $p < 0.01$ ). However, it was significantly  
21 lower to 62.71 mg/dL in PLGA-Oltipraz group compare to BUN content in Oltipraz group ( $p <$   
22  $0.05$ ) (Fig. 5d). The creatinine showed 1.98 mg/dL in PBS and 1.75 mg/dL in PLGA added control  
23 cells, while 1.46 mg/dL in Oltipraz and 1.03 mg/dL in PLGA-Oltipraz treated cells during hypoxia.  
24 The creatinine level in PLGA-Oltipraz treated cells was decreased compared to that in PLGA  
25 treated cells ( $p < 0.05$ ). Moreover, it was significantly lower in PLGA-Oltipraz group compared to

1 creatinine in Oltipraz group ( $p < 0.05$ ) (Fig. 5e). The results suggest that the PLGA-Oltipraz NPs  
 2 are effective on protecting renal function at the initial phase of AKI. Overall, we demonstrated that  
 3 at the initial phase of renal IR injury, PLGA-Oltipraz NPs (100 nm) passed through the impaired  
 4 GFB, accumulated in renal tubules and were taken up by renal tubular epithelial cells. Then,  
 5 Oltipraz were gradually released from the NPs, activating the expression of anti-oxidative stress-  
 6 related Nrf2 and its downstream targets NQO1, GCLC, and Gpx2, which reduced the tubular  
 7 damage and alleviated renal fibrosis.



1 **Figure 5. Histological analysis of the IR kidneys.** (a) IR kidneys on day 3 after RIRI were  
 2 prepared and analyzed. Representative images and histological score of H&E and Masson staining  
 3 in each group. (b) After 6 weeks, injury kidneys were collected and prepared for histological  
 4 analysis. Representative images and histological score of H&E and Masson staining in each group.  
 5 (c) Western blot analysis of protein levels of Nrf2 and downstream NQO1, GCLC and Gpx2 in IR  
 6 mice on days 3 and 7 after RIRI. (d) Blood urea nitrogen (BUN) level and (e) creatinine levels at  
 7 24 h in mice with and without AKI. The data are shown as mean  $\pm$  SD (n=3). \*P<0.05, \*\*P<0.01,  
 8 n.s., not significant, t test.



9

1 **Figure 6. Histological analysis of the IR kidneys.** (a) IR kidneys on day 3 after RIRI were  
2 prepared and analyzed. IHC staining and the corresponding percentage of positive areas of  $\alpha$ -SMA,  
3 collagen I, and fibronectin. Scale bar, 100  $\mu$ m. (b) After 6 weeks, injury kidneys were collected and  
4 prepared for histological analysis. IHC staining and the corresponding percentage of positive areas  
5 of  $\alpha$ -SMA, collagen I, and fibronectin. Scale bar, 100  $\mu$ m. The data are shown as mean  $\pm$  SD (n=3).  
6 \*P<0.05, \*\*P<0.01, \*\*\*P<0.001, t test.

7  
8 We further evaluated the potential toxicity of PLGA NPs on major organs (heart, liver, spleen,  
9 and lung) after RIRI (Figure S2). We harvested the major organs from sham-operated and RIRI  
10 mice treated with PBS, PLGA, single Oltipraz and PLGA-Oltipraz NPs. H&E-stained sections of  
11 the four tissues (heart, liver, spleen and lung) showed no apparent lesions (no necrosis, edema,  
12 inflammatory infiltration and hyperplasia) in either group. Thus, PLGA-Oltipraz NPs  
13 administration did not induce significant damage to major organs.

14  
15 Currently no effective treatment is available for AKI in clinic even after investigating for  
16 decades. Instead of developing more effective agents, many efforts were made by improving the  
17 treatment strategies with nanotechnology. The GFB becomes the greatest barrier to deliver agents  
18 to renal tubules. Though newly designed nanoparticles could pass through GFB and target to the  
19 renal tubules, they were still far away from clinical application. In the present study, we found a  
20 “therapeutic window” during AKI, which enable us to effectively deliver agents to renal tubular  
21 epithelial cells with FDA approved starting materials.

#### 22 23 **4. Conclusion**

24 In summary, we fabricated biocompatible PGLA-based Oltipraz NPs with the ability of forming  
25 high accumulation in the IR kidney and targeting renal tubules for treating IR-induced AKI. PLGA-

1 Oltipraz NPs represent a passive target route for injured kidneys after RIRI with strict particle-size  
2 selection. The high NPs accumulation in IR kidneys enables concentrated release of encapsulated  
3 drugs *in situ* to alleviate the inflammatory damage caused by IR and reduce renal fibrosis. The  
4 designed NPs could be a promising treatment strategy for IR-induced AKI and significant potential  
5 in clinical translation can be predicted.

## 6 **Associated content**

## 7 **Supporting Information**

8 The Supporting Information (SI) includes histological analysis of the kidneys after sham surgery  
9 and treatment, and histological analysis of the major organs at 6 weeks after RIRI model and  
10 treatment (Figure S1-S2).  
11

## 12 **Acknowledgment**

13 This work was supported by grants from the Project of Technology and Education Jiangsu  
14 Provincial Key Medical Discipline QNRC2016015 (to X.Z.), Invigorating Health Care through  
15 Science ZDXKB2016014 (to H.G.), China Postdoctoral Science Foundation 2018M640477 (to  
16 X.Z.), Nanjing Health Distinguished Youth Fund JQX15006 (to X.Z.), Nanjing Science and  
17 Technology Project 201715025 (to X.Z.).  
18

## 19 **Notes**

20 The authors declare no competing financial interest.  
21

## 22 **References**

23 [1] E.A.J. Hoste, J.A. Kellum, N.M. Selby, A. Zarbock, P.M. Palevsky, S.M. Bagshaw, et al.,  
24 Global epidemiology and outcomes of acute kidney injury, *Nat. Rev. Nephrol.* 14 (2018) 607-  
25

- 1 625.
- 2 [2] A. Zuk, J.V. Bonventre, Acute Kidney Injury, *Annu. Rev. Med.* 67 (2016) 293-307.
- 3 [3] N.H. Lameire, A. Bagga, D. Cruz, J. De Maeseneer, Z. Endre, J.A. Kellum, et al., Acute kidney  
4 injury: an increasing global concern, *Lancet* 382 (2013) 170-179.
- 5 [4] E.A. Hoste, S.M. Bagshaw, R. Bellomo, C.M. Cely, R. Colman, D.N. Cruz, et al.,  
6 Epidemiology of acute kidney injury in critically ill patients: the multinational AKI-EPI study,  
7 *Intensive. Care. Med.* 41 (2015) 1411-1423.
- 8 [5] D.A. Ferenbach, J.V. Bonventre, Mechanisms of maladaptive repair after AKI leading to  
9 accelerated kidney ageing and CKD, *Nat. Rev. Nephrol.* 11 (2015) 264-276.
- 10 [6] M. Matejovic, C. Ince, L.S. Chawla, R. Blantz, B.A. Molitoris, M.H. Rosner, et al., Renal  
11 Hemodynamics in AKI: In Search of New Treatment Targets, *J. Am. Soc. Nephrol.* 27 (2016)  
12 49-58.
- 13 [7] B.C. Liu, T.T. Tang, L.L. Lv, H.Y. Lan, Renal tubule injury: a driving force toward chronic  
14 kidney disease, *Kidney Int.* 93 (2018) 568-579.
- 15 [8] K.C. Leung, M. Tonelli, M.T. James, Chronic kidney disease following acute kidney injury-  
16 risk and outcomes, *Nat. Rev. Nephrol.* 9 (2013) 77-85.
- 17 [9] M.U. Sharif, M.E. Elsayed, A.G. Stack, The global nephrology workforce: emerging threats  
18 and potential solutions!, *Clin. Kidney J.* 9 (2016) 11-22.
- 19 [10] N. Kamaly, J.C. He, D.A. Ausiello, O.C. Farokhzad, Nanomedicines for renal disease: current  
20 status and future applications, *Nat. Rev. Nephrol.* 12 (2016) 738-753.
- 21 [11] R.M. Williams, E.A. Jaimes, D.A. Heller, Nanomedicines for kidney diseases, *Kidney Int.* 90  
22 (2016) 740-745.
- 23 [12] G.T. Tietjen, S.A. Hosgood, J. DiRito, J. Cui, D. Deep, E. Song, et al., Nanoparticle targeting to  
24 the endothelium during normothermic machine perfusion of human kidneys, *Sci. Transl. Med.*  
25 9 (2017).

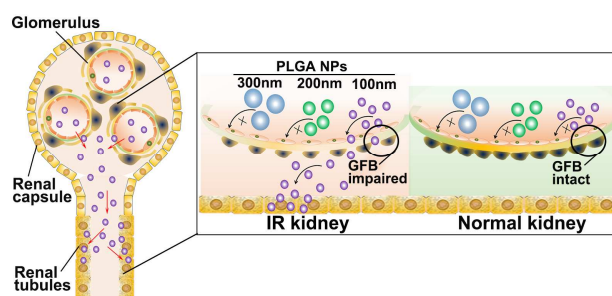
- 1 [13]J. Wang, J.J. Masehi-Lano, E.J. Chung, Peptide and antibody ligands for renal targeting:  
2 nanomedicine strategies for kidney disease, *Biomater. Sci.* 5 (2017) 1450-1459.
- 3 [14]R.M. Williams, J. Shah, B.D. Ng, D.R. Minton, L.J. Gudas, C.Y. Park, et al., Mesoscale  
4 nanoparticles selectively target the renal proximal tubule epithelium, *Nano Lett.* 15 (2015)  
5 2358-2364.
- 6 [15]S. Gao, S. Hein, F. Dagnaes-Hansen, K. Weyer, C. Yang, R. Nielsen, et al., Megalin-mediated  
7 specific uptake of chitosan/siRNA nanoparticles in mouse kidney proximal tubule epithelial  
8 cells enables AQP1 gene silencing, *Theranostics* 4 (2014) 1039-1051.
- 9 [16]M.G. Lawrence, M.K. Altenburg, R. Sanford, J.D. Willett, B. Bleasdale, B. Ballou, et al.,  
10 Permeation of macromolecules into the renal glomerular basement membrane and capture by  
11 the tubules, *Proc. Natl. Acad. Sci. U S A* 114 (2017) 2958-2963.
- 12 [17]C. von Roemeling, W. Jiang, C.K. Chan, I.L. Weissman, B.Y.S. Kim, Breaking Down the  
13 Barriers to Precision Cancer Nanomedicine, *Trends Biotechnol.* 35 (2017) 159-171.
- 14 [18]S. Satchell, The role of the glomerular endothelium in albumin handling, *Nat. Rev. Nephrol.* 9  
15 (2013) 717-725.
- 16 [19]S. Alidori, N. Akhavein, D.L. Thorek, K. Behling, Y. Romin, D. Queen, et al., Targeted fibrillar  
17 nanocarbon RNAi treatment of acute kidney injury, *Sci. Transl. Med.* 8 (2016) 331-339.
- 18 [20]H. Qiao, M. Sun, Z. Su, Y. Xie, M. Chen, L. Zong, et al., Kidney-specific drug delivery system  
19 for renal fibrosis based on coordination-driven assembly of catechol-derived chitosan,  
20 *Biomaterials* 35 (2014) 7157-7171.
- 21 [21]D. Jiang, Z. Ge, H.J. Im, C.G. England, D. Ni, J. Hou, et al., DNA origami nanostructures can  
22 exhibit preferential renal uptake and alleviate acute kidney injury, *Nat. Biomed. Eng.* 2 (2018)  
23 865-877.
- 24 [22]M. Malek, M. Nematbakhsh, Renal ischemia/reperfusion injury; from pathophysiology to  
25 treatment, *J. Renal. Inj. Prev.* 4 (2015) 20-27.

- 1 [23]M. Andersson, U. Nilsson, C. Hjalmarsson, B. Haraldsson, J.S. Nystrom, Mild renal ischemia-  
2 reperfusion reduces charge and size selectivity of the glomerular barrier, *Am. J. Physiol. Renal.*  
3 *Physiol.* 292 (2007) 1802-1809.
- 4 [24]S.I. Tyritzis, M. Zachariades, K. Evangelou, V.G. Gorgoulis, A. Kyroudi-Voulgari, K. Pavlakis,  
5 et al., Effects of prolonged warm and cold ischemia in a solitary kidney animal model after  
6 partial nephrectomy: an ultrastructural investigation, *Ultrastruct Pathol.* 35 (2011) 60-65.
- 7 [25]C. Rippe, A. Rippe, A. Larsson, D. Asgeirsson, B. Rippe, Nature of glomerular capillary  
8 permeability changes following acute renal ischemia-reperfusion injury in rats, *Am. J. Physiol.*  
9 *Renal. Physiol.* 291 (2006) 1362-1368.
- 10 [26]L.M. Shelton, B.K. Park, I.M. Copple, Role of Nrf2 in protection against acute kidney injury,  
11 *Kidney Int.* 84 (2013) 1090-1095.
- 12 [27]M. Nezu, T. Souma, L. Yu, T. Suzuki, D. Saigusa, S. Ito, et al., Transcription factor Nrf2  
13 hyperactivation in early-phase renal ischemia-reperfusion injury prevents tubular damage  
14 progression, *Kidney Int.* 91 (2017) 387-401.
- 15 [28]S. Ruiz, P.E. Pergola, R.A. Zager, N.D. Vaziri, Targeting the transcription factor Nrf2 to  
16 ameliorate oxidative stress and inflammation in chronic kidney disease, *Kidney Int.* 83 (2013)  
17 1029-1041.
- 18 [29]J.M. Chan, L. Zhang, K.P. Yuet, G. Liao, J.W. Rhee, R. Langer, et al., PLGA-lecithin-PEG  
19 core-shell nanoparticles for controlled drug delivery, *Biomaterials* 30 (2009) 1627-1634.
- 20 [30]L. Zhang, J.M. Chan, F.X. Gu, J.W. Rhee, A.Z. Wang, A.F. Radovic-Moreno, et al., Self-  
21 assembled lipid-polymer hybrid nanoparticles: a robust drug delivery platform, *ACS Nano* 2  
22 (2008) 1696-1702.
- 23 [31]B. Tampe, U. Steinle, D. Tampe, J.L. Carstens, P. Korsten, E.M. Zeisberg, et al., Low-dose  
24 hydralazine prevents fibrosis in a murine model of acute kidney injury-to-chronic kidney  
25 disease progression, *Kidney Int.* 91 (2017) 157-176.

- 1 [32]L. Ge, W. Chen, W. Cao, G. Liu, Q. Zhang, J. Zhuang, et al., GCN2 is a potential prognostic  
2 biomarker for human papillary renal cell carcinoma, *Cancer Biomark.* 22 (2018) 395-403.
- 3 [33]C. Yuste, E. Gutierrez, A.M. Sevillano, A. Rubio-Navarro, J.M. Amaro-Villalobos, A. Ortiz, et  
4 al., Pathogenesis of glomerular haematuria, *World J. Nephrol.* 4 (2015) 185-195.
- 5 [34]H. Castrop, I.M. Schiessl, Novel routes of albumin passage across the glomerular filtration  
6 barrier, *Acta. Physiol. (Oxf)* 219 (2017) 544-553.
- 7 [35]W. Wang, G. Ramesh, Segment-specific expression of netrin-1 receptors in normal and  
8 ischemic mouse kidney, *Am. J. Nephrol.* 30 (2009) 186-193.
- 9 [36]Q. Ma, Role of nrf2 in oxidative stress and toxicity, *Annu. Rev. Pharmacol Toxicol* 53 (2013)  
10 401-426.
- 11 [37]M.S. Joo, C.G. Lee, J.H. Koo, S.G. Kim, miR-125b transcriptionally increased by Nrf2 inhibits  
12 AhR repressor, which protects kidney from cisplatin-induced injury, *Cell Death Dis.* 4 (2013)  
13 e899.
- 14 [38]A. Atilano-Roque, X. Wen, L.M. Aleksunes, M.S. Joy, Nrf2 activators as potential modulators  
15 of injury in human kidney cells, *Toxicol Rep.* 3 (2016) 153-159.
- 16 [39]W. Kong, J. Fu, N. Liu, C. Jiao, G. Guo, J. Luan, et al., Nrf2 deficiency promotes the  
17 progression from acute tubular damage to chronic renal fibrosis following unilateral ureteral  
18 obstruction, *Nephrol. Dial. Transplant* 33 (2018) 771-783.
- 19 [40]M.J. Moeller, V. Tenten, Renal albumin filtration: alternative models to the standard physical  
20 barriers, *Nat. Rev. Nephrol.* 9 (2013) 266-277.
- 21 [41]M. Liu, N.M. Reddy, E.M. Higbee, H.R. Potteti, S. Noel, L. Racusen, et al., The Nrf2  
22 triterpenoid activator, CDDO-imidazolide, protects kidneys from ischemia-reperfusion injury  
23 in mice, *Kidney Int.* 85 (2014) 134-141.

24

25

1 **TOC Graphic:**

2

3 Design of size-selective PLGA-Oltipraz nanoparticles for effective treatment of ischemia-  
4 reperfusion (IR) induced acute kidney injury (AKI).

5

**CRedit author statement**

**Hang Yu:** Conceptualization, Methodology, Data curation. **Tingsheng Lin:** Conceptualization, Methodology, Software, Writing- Original draft preparation. **Wei Chen:** Visualization, Investigation, Writing- Reviewing and Editing, Supervision. **Wenmin Cao:** Methodology, Data curation, Validation. **Chengwei Zhang:** Methodology, Software, Formal Analysis. **Tianwei Wang:** Methodology, Data curation. **Meng Ding:** Writing- Reviewing and Editing, Supervision. **Sheng Zhao:** Writing- Reviewing and Editing. **Hui Wei:** Conceptualization, Writing- Reviewing and Editing. **Hongqian Guo:** Conceptualization, Supervision, Project Administration, Funding Acquisition. **Xiaozhi Zhao:** Conceptualization, Supervision, Project Administration, Funding Acquisition.

The above descriptions are accurate and agreed by all authors.